# Suppression of stimulated Raman scattering by angularly incoherent light, towards a laser system of incoherence in all dimensions of time, space, and angle

Yi Guo; Xiaomei Zhang **∑**; Dirui Xu; ... et. al



Matter and Radiation at Extremes 8, 035902 (2023) https://doi.org/10.1063/5.0136567





Citation

CrossMark

### Articles You May Be Interested In

An angular-resolved scattered-light diagnostic for laser-plasma instability studies

Rev Sci Instrum (May 2022)

Optoelectronic simulation of GaAs solar cells with angularly selective filters

Journal of Applied Physics (February 2014)

The importance of nuclear spin diffusion as an angularly independent relaxation mechanism controlling the matrix ENDOR response of radicals in molecular crystals

J. Chem. Phys. (January 1981)







## Suppression of stimulated Raman scattering by angularly incoherent light, towards a laser system of incoherence in all dimensions of time, space, and angle

Cite as: Matter Radiat. Extremes 8, 035902 (2023); doi: 10.1063/5.0136567 Submitted: 27 November 2022 • Accepted: 21 March 2023 •







Published Online: 25 April 2023

Yi Guo, Dirui Xu, Dirui Xu







#### **AFFILIATIONS**

- Department of Physics, Shanghai Normal University, Shanghai 200234, China
- Institute of Applied Physics and Computational Mathematics, Beijing 100094, China

#### **ABSTRACT**

Laser-plasma instability (LPI) is one of the main obstacles to achieving predictable and reproducible fusion at high gain through laser-driven inertial confinement fusion (ICF). In this paper, for the first time, we show analytically and confirm with three-dimensional particle-incell simulations that angular incoherence provides suppression of the instability growth rate that is additional to and much stronger than that provided by the well-known temporal and spatial incoherence usually used in ICF studies. For the model used in our calculations, the maximum field ratio between the stimulated Raman scattering and the driving pulses drops from 0.2 for a Laguerre-Gaussian pulse with a single nonzero topological charge to 0.05 for a super light spring with an angular momentum spread and random relative phases. In particular, angular incoherence does not introduce extra undesirable hot electrons. This provides a novel method for suppressing LPI by using light with an angular momentum spread and paves the way towards a low-LPI laser system for inertial fusion energy with a super light spring of incoherence in all dimensions of time, space, and angle, and may open the door to the use of longer-wavelength lasers for inertial fusion energy.

© 2023 Author(s). All article content, except where otherwise noted, is licensed under a Creative Commons Attribution (CC BY) license (http://creativecommons.org/licenses/by/4.0/). https://doi.org/10.1063/5.0136567

Laser plasma instabilities (LPIs), 1-3 in the form, for example, of stimulated Raman scattering (SRS), stimulated Brillouin scattering (SBS), or two-plasmon decay (TPD), are fundamental limiters of fusion performance for all approaches to laser-driven inertial confinement fusion (ICF), 4-6 because they may cause significant laser energy loss, generate undesirable hot electrons,<sup>5</sup> and seriously influence the drive symmetry on the target. Thus, mitigation of LPI effects is crucial for achieving predictable and reproducible fusion at high gain in the progress toward the practical realization of inertial fusion energy. To suppress LPI for ICF, it has been proposed that the instability growth rate in the plasma could be reduced by either temporal or spatial incoherence of the driving laser. This is because the incoherence of a laser can be understood as a superimposition of temporal and spatial modes, which changes the amplitude a or intensity  $a^2$  of the laser in time or space. We know that the total laser energy can be written as  $\propto \int a^2 dt$ ,

while the total instability growth in the linear region can be written as  $\propto \int adt$ . Thus, for a given total laser energy, a laser with a changing amplitude exhibits less total instability growth. The effect of incoherence in suppressing LPI can also be explained in another way. For two given stimulated waves, such as a plasma wave and a scattering wave, only one mode of the driving laser can couple with them exactly resonantly, while the others contribute less to the instability growth rate. Therefore, for a given average laser intensity, an incoherent laser has a lower instability growth rate. To date, many methods have been proposed to suppress LPI using spatial and temporal incoherence in the driving lasers, through, for example, laser smoothing techniques 14-18 and broadband laser technology. 15 the latter in particular, both theoretical and experimental results indicate that the linear growth of LPI can be controlled well when the laser bandwidth is much larger than the growth rate. 23,24 Meanwhile, decoupled broadband lasers 13,25-27 or polychromatic lights

a) Authors to whom correspondence should be addressed: zhxm@shnu.edu.cn and bfshen@shnu.edu.cn

composed of multiple colors of beamlets <sup>10,28</sup> show better inhibitory effects than continuous broadband lasers.

Even with these methods, the SRS of the inner laser beams at the National Ignition Facility (NIF)<sup>1,12,29–31</sup> remains a major problem for high-convergence implosion with a CH capsule inside a gasfilled hohlraum driven by a long laser pulse. 32-34 The inner beams of the NIF hohlraums have a long propagation path and encounter plasma blowoff from the high-Z walls, low-Z plasma ablated from the capsule, and any filling gas within the hohlraum, which results eventually in unpredictable and serious SRS. With the aim of achieving a low level of LPI, attention has turned to the use of ablators made of high-density carbon (HDC), which has the advantage of high density, allowing the use of thinner capsules and shorter laser pulses and thus leading to a low level of LPI and better symmetry control in low gas-filled hohlraums. With an HDC capsule, the recent tremendous breakthrough of 3.15 MJ fusion yield from 2.05 MJ energy input on the NIF has provided a successful demonstration of ignition in ICF.35 Nevertheless, the NIF results demonstrate that there is a limit on the degree to which LPI can be reduced via both temporal incoherence and spatial incoherence, and suppression of SRS is still a crucial task if the NIF is to be able to achieve a predictable and reproducible fusion gain via a low-entropy and high-convergence implosion driven by a long laser pulse.

Given that the temporal and spatial dimensions are related to energy (frequency) and momentum, while the angular dimension is related to angular momentum, it should be possible to suppress LPI via angular incoherence. The spatial coherence area is usually expressed as the product of two spatial lengths, that is,  $\Delta s = \Delta y \cdot \Delta z$ for a laser propagating in the x direction. We can rewrite this as  $\Delta s = r \Delta r \Delta \varphi$ . In this way,  $\Delta r$  is related to radial coherence and  $\Delta \varphi$ to angular coherence. Taking SRS as an example, we know that SRS in plasma is a three-wave coupling process related to the decay of a driving laser into an electron plasma wave and a scattering wave, in which the following frequency and wave number matching corresponding to energy and momentum conservation must be satisfied:  $\omega_L = \omega_1 + \omega_2$  and  $\mathbf{k}_L = \mathbf{k}_1 + \mathbf{k}_2$ . In addition to energy and momentum, the driving laser may also carry angular momentum, in which case angular momentum conservation must also be satisfied for the LPI, that is,  $L_L = L_1 + L_2$ . In fact, the presence of orbital angular momentum in the driving laser beam (such as in a Laguerre-Gaussian beam) has been used to study Raman scattering in laser-plasma interaction. 36-39 In this paper, we propose for the first time to suppress LPI with angularly incoherent light and pay particular attention to the effect of angular incoherence on the instability growth rate, which should pave the way towards a low-LPI laser system with a super light spring of incoherence in all dimensions of time, space, and angle. We prove analytically and with three-dimensional (3D) particle-in-cell (PIC) simulations that angular incoherence provides suppression of the instability growth rate that is additional to and much stronger than that provided by temporal incoherence.

A good description of the radial and angular momenta of the driving laser can be given using the Laguerre–Gaussian modes

$$a_L(x,t) = a_n \exp \left[ i\omega_L t - ik_L x + il_L \varphi + \phi \right], \tag{1}$$

where  $a_n$  is the transverse profile,  $\omega_L$  is the laser frequency,  $k_L = 2\pi/\lambda_L$  is the wave number,  $l_L$  is the topological charge,

 $\varphi = \tan^{-1}(z/y)$ , and  $\phi$  is the original phase at the waist plane. The transverse profile  $a_n$  is given by

$$a_n = a_0 (-1)^p \frac{C_{pl}}{w(x)} \left[ \frac{\sqrt{2}r}{w(x)} \right]^{|l|} \exp \left[ -\frac{r^2}{w(x)^2} \right] L_p^{|l|} \left( \frac{2r^2}{w(x)^2} \right),$$

where  $a_0$  is the normalized amplitude,  $C_{pl}$  is a normalization constant,  $w(x) = w_0 \sqrt{1 + x^2/x_R^2}$  [where  $x_R$  is the Rayleigh length  $R_x = (x^2 + x_R^2)/x$  and  $w_0$  is the beam-waist radius],  $r = \sqrt{y^2 + z^2}$ , is the associated Laguerre polynomial, and p is the number of radial nodes in the intensity distribution. In this paper, we concentrate on studying the effect of angular incoherence, and therefore we set  $p \equiv 0$ .

Here, we consider a specific case. The driving laser is a superimposition of N modes of different frequency  $\omega_L$  and topological charge  $l_L$ . The laser amplitude is written as

$$a_L(x,t) = \sum_{n=0}^{N-1} a_n \exp\left[i\omega_{Ln}t - ik_{Ln}x + il_{Ln}\varphi + \phi_n\right]. \tag{2}$$

For simplicity, we assume  $a_n \equiv a_0$ . The frequencies  $\omega_{Ln} = 1 + n\varepsilon_1\omega_{L0}$ of the modes have the same interval  $\varepsilon_1\omega_{L0}$ , and the total bandwidth is  $\Delta \omega = (N-1)\varepsilon_1\omega_{L0}$ , where  $\omega_{L0}$  is the frequency of the first mode and  $\varepsilon_1$  is a constant that indicates the bandwidth gap. Usually,  $\Delta \omega / \omega_{L0} \ll 1$ . The charges  $l_{Ln} = 1 + n\varepsilon_2 l_{L0}$  and the total topological charge spread  $\Delta l = (N-1)\varepsilon_2 l_{L0}$ , where  $l_{L0}$  is the topological charge corresponding to the first mode and  $\epsilon_2$  is a constant that indicates the topological charge gap. Typically,  $\varepsilon_2 l_{L0}$  is an integer. If  $\phi_n \equiv 0$ , the structure of such a laser is called a light spring. 40,41 Thus, the distribution of the highest intensities, that is, the strong point, resembles a spring. In this paper, we call a light spring with random phases  $\phi_n$  a super light spring. Hereinafter, for simplicity, a laser with Laguerre-Gaussian modes is referred to as an LG laser, and a laser with a light spring or super light spring structure is referred to as an LS or super LS laser. Owing to superimposition, the amplitude for  $\phi_n \equiv 0$  can be written as

$$a_L(x,r,\varphi,t) = a_0(r) \frac{\sin\left[N(\varepsilon_1\omega_{L0}t - \varepsilon_1k_{L0}x - \varepsilon_2l_{L0}\varphi)/2\right]}{\sin\left[(\varepsilon_1\omega_{L0}t - \varepsilon_1k_{L0}x - \varepsilon_2l_{L0}\varphi)/2\right]}.$$
 (3)

This implies that the angular spread is reduced to  $2\pi/N$ , and the angular position of the highest intensity can be written as  $\varphi_{\max} = \varepsilon_1 \omega_{L0} t/(\varepsilon_2 l_{L0})$ . By changing  $\varphi$  from 0 to  $2\pi$ , we can obtain the pitch of an LS laser.

SRS of a nonrelativistic laser can be described by 42,43

$$\left(\frac{\partial^2}{\partial t^2} - c^2 \nabla^2 + \omega_{pe}^2\right) \tilde{\boldsymbol{a}} = -\tilde{n}_e \mathbf{a}_L, \tag{4}$$

$$\left(\frac{\partial^2}{\partial t^2} + \omega_{pe}^2 - 3\nu_e^2 \nabla^2\right) \tilde{n}_e = n_0 \nabla^2 (\mathbf{a}_L \cdot \tilde{\mathbf{a}}), \tag{5}$$

where  $\omega_{pe}$  is the electron plasma frequency,  $\mathbf{a}_L$  is the vector potential of the driving laser pulse,  $\tilde{\mathbf{a}}$  is the vector potential of the backscattered wave,  $\tilde{n}_e$  is the plasma density perturbation, and  $n_0 = \omega_{pe}^2/4\pi e$ . We neglect the radial gradient (this is reasonable for a sufficiently large focal spot) and consider that a wave of the form

 $\sim \exp(i\omega t - ikx + il\phi)$  is excited. For the scattered wave of lower frequency, we have

$$\omega^{2} - \omega_{l}^{2} = \frac{k_{l}^{2} c^{2} \omega_{pe}^{2} a_{0}^{2}}{4} \times \sum_{n=0}^{N-1} \frac{1}{(\omega - \omega_{Ln})^{2} - (k - k_{Ln})^{2} c^{2} - c^{2} (l - l_{Ln})^{2} / r^{2} - \omega_{pe}^{2}},$$
(6)

where  $\omega_l = \left[\omega_{pe}^2 + 3v_e^2\left(k^2 + l^2/r^2\right)\right]^{1/2}$  is the Langmuir wave frequency and  $k_l^2 = k^2 + l^2/r^2$ . Note that the dispersion relation depends on the radial position r. For simplicity, we discuss the dispersion relations at radius R of the highest intensity for the LG and LS pulses.

Note that only one laser mode is exactly resonant. Denoting the resonant mode by  $(\omega_{L0}, l_{L0}, l_{L0})$ , we obtain

$$(\omega_l - \omega_{L0})^2 - (k - k_{L0})^2 c^2 - (l - l_{L0})^2 c^2 / R^2 - \omega_{pe}^2 = 0.$$
 (7)

We write  $\omega = \omega_l + \delta \omega = \omega_l + i \gamma_s$ , with  $\delta \omega \ll \omega_l$ . For simplicity, we ignore the effect of wave vector matching.

First, we discuss the case of  $\varepsilon_2 = 0$ . We have

$$\gamma_s^2 \approx \frac{k_1^2 c^2 a_0^2}{16} \frac{\omega_{pe}^2}{\omega_l \omega_{s0}} \sum_{n=0}^{N-1} \frac{1}{1 + (n\varepsilon_1 \omega_{L0})^2 / \gamma_s^2},$$
 (8)

where  $\omega_{s0} = \omega_{L0} - \omega_l$  is the frequency of the backward SRS beam. When  $n\varepsilon_1\omega_{L0} \ll \gamma$ , we obtain the following expression for the instability growth rate  $\gamma_s$ :

$$\gamma_s \approx \frac{k_l c a_0}{4} \left( \frac{\omega_{pe}^2}{\omega_l \omega_{s0}} \right)^{1/2} \sqrt{N} \left[ 1 - \frac{\left( N \varepsilon_1 \omega_{L0} \right)^2}{3 \gamma_s^2} \right]^{1/2} \approx \gamma_0 \left[ 1 - \frac{\left( \Delta \omega \right)^2}{6 \gamma_s^2} \right],$$

where  $\gamma_0 = \sqrt{N} (k_l c a_0/4) (\omega_{pe}^2/\omega_l \omega_{s0})^{1/2}$  is the growth rate without spreading. Equation (9) means that a larger bandwidth is better for suppressing SRS.

We now discuss the case of  $\varepsilon_1=0$ . We assume that orbital angular momentum is not transferred to the electron plasma wave and that  $n\varepsilon_2 l_{L0}^2 c^2/R^2 \ll \omega_I \omega_{s0}$ . We have

$$\gamma_s^2 \approx \frac{k_f^2 c^2 a_0^2}{16} \frac{\omega_{pe}^2}{\omega_l \omega_{s0}} \sum_{n=0}^{N-1} \frac{1}{1 + \left(n \varepsilon_2 l_{10}^2 c^2 / \omega_{s0} \gamma_s R^2\right)^2}.$$
 (10)

When  $n\varepsilon_2 l_{L0}^2 c^2/R^2 \ll \omega_{s0} \gamma_s$ , we obtain the following expression for the instability growth rate  $\gamma_c$ :

$$\gamma_{s} \approx \frac{k_{l}ca_{0}}{4} \left(\frac{\omega_{pe}^{2}}{\omega_{l}\omega_{s0}}\right)^{1/2} \sqrt{N} \left[1 - \frac{1}{3} \left(\frac{N\varepsilon_{2}l_{L0}^{2}c^{2}}{\omega_{s0}\gamma_{s}R^{2}}\right)^{2}\right]^{1/2}$$

$$\approx \gamma_{0} \left[1 - \frac{1}{6} \left(\frac{l_{L0}\Delta lc^{2}}{\omega_{s0}\gamma_{s}R^{2}}\right)^{2}\right]. \tag{11}$$

Here, we assume that  $\Delta \omega/\omega_{L0} \ll 1$  and  $\Delta l/l_{L0} \ll 1$ , which are reasonable assumptions to obtain the approximate growth rate.

For an actual superimposed laser pulse, the peak laser amplitude is  $Na_0$ . Therefore, the present formulas for the growth rate is the same as before except for the correction term

 $(l_{L0}\Delta lc^2)^2/6(\omega_{s0}\gamma_sR^2)^2$ . According to Eqs. (9) and (11), we can see that there are two correction terms that can reduce the instability growth rate. One is the total bandwidth  $\Delta\omega$ , which has been widely investigated in ICF. The other is the total topological charge spread  $\Delta l$ . Note that at  $\Delta l > (1/l_{L0})(\omega_{s0}/\omega_{L0})(2\pi R/\lambda_{L0})^2(\Delta\omega/\omega_{L0})$ , the  $\Delta l$  term will dominate the correction term, and hence the spread of angular momentum plays a more important role than the bandwidth in suppressing  $\gamma_s$ . Because  $\Delta\omega/\omega_{L0} \ll 1$ , it is easy to realize  $\Delta l > (1/l_{L0})(\omega_{s0}/\omega_{L0})(2\pi R/\lambda_{L0})^2(\Delta\omega/\omega_{L0})$  for a real superimposed laser pulse.

To confirm the above analysis, we perform 3D PIC simulations using the POCH code.<sup>44</sup> In all simulations, we set  $\varepsilon_2 l_{L0}$  = 1. To reduce the simulation time, we take  $l_{L0}$  = 3 and N = 7, resulting in an average topological charge  $\bar{l}$  = 6. Note that a much larger  $l_{L0}$  can be used in a real experiment. For simplicity, we consider the same transverse profile for each mode in Eq. (2):

$$a_n \equiv a_0 = a_{00} \left( \frac{\sqrt{2}r}{w_0} \right)^{l_{L0}} \exp\left( -\frac{r^2}{w_0^2} \right).$$

To further reduce the simulation time, we choose a large amplitude  $a_{00} = 0.06$ ,  $w_0 = 10 \ \mu \text{m}$ . The central laser wavelength is  $\lambda_{Lc} = 0.8 \ \mu \text{m}$  and the corresponding central frequency is  $\omega_{Lc} = 3.75 \times 10^{14} \text{ Hz}$ . The frequency of the first mode is  $\omega_{L0} = 3.4125 \times 10^{14} \text{ Hz}$  ( $\omega_{L0} = 0.91 \omega_{Lc}$ ).

Therefore, the power of the LS pulse is P = 0.16 TW. The frequency separation  $\varepsilon_1 \omega_{L0} = 0.03 \omega_{Lc} = 0.033 \omega_{L0}$  ( $\varepsilon_1 = 0.033$ ), and thus the total frequency spread is  $(N-1)\varepsilon_1\omega_{L0} = 0.198\omega_{L0}$ . With this, we obtain a pitch  $\Delta x = 2\pi c/(\varepsilon_1 \omega_{L0}) \approx 27 \ \mu \text{m}$  for the LS pulse. The laser has a constant amplitude in time, with a duration of about 93.3 fs. The plasma density in the simulation is  $n_e = 1.7 \times 10^{20} \text{ cm}^{-3}$ . The size of the simulation box is 60  $\mu$ m (x) × 80  $\mu$ m (y) × 80  $\mu$ m (z), corresponding to a moving window of 600 × 800 × 800 cells, with one particle per cell. The plasma occupies the 15  $\mu$ m < x < 800  $\mu$ m region in the direction of the laser pulse propagation, and  $-75 \mu m$  $< y < 75 \mu \text{m}, -75 \mu \text{m} < z < 75 \mu \text{m}$ . It should be noted here that we consider a plasma with a relatively high density to ensure that the scattered wave can be separated from the driving wave completely in spectral space and then filtered out for mathematical analysis. Actually, the angular coherence as well as the temporal and spatial coherences are characteristics of the light, and the suppression of SRS for an LS laser with angular incoherence also works in a low-density plasma.

Figure 1(a) shows the 2D k-space distribution of the driving laser pulse after propagation for 240  $\mu$ m. As can be seen, the LS pulse is composed of seven separated frequencies, and the weak signal on the left side of the driving laser is Raman scattering. For comparison, we consider a broadband LG laser pulse, which is a superimposition of N modes with different frequencies but the same topological charge  $\bar{l}$ , that is, with a spread of  $\varepsilon_2 l_{L0} = 0$  for the angular momentum. The total power and other parameters remain the same as those for the above LS pulse. Figure 1(b) shows the 2D k-space distribution for the LG case, again after the pulse has propagated 240  $\mu$ m. Clearly, there is a much stronger SRS signal in the LG case, which confirms the above theoretical expectation that the  $\Delta l$  incoherence

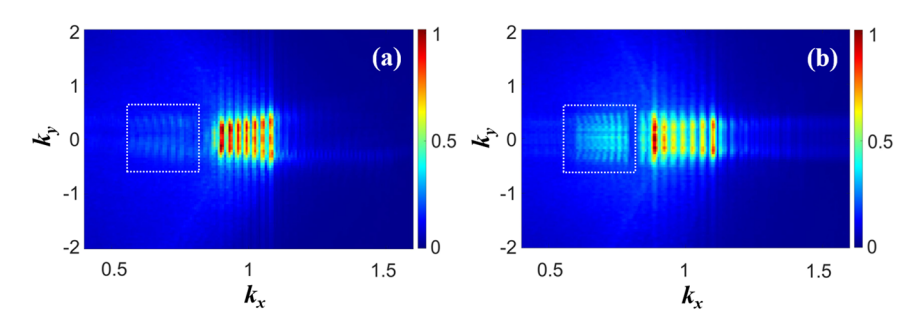


**FIG. 1.** Spectral distributions in k space when the driving laser pulse reaches  $x=240~\mu\mathrm{m}$  for (a) an LS pulse with topological charge varying from l=3 to l=9 and total bandwidth  $\Delta\omega=0.198\omega_{L0}$  and (b) an LG pulse with topological charge l=6 and bandwidth  $\Delta\omega=0.198\omega_{L0}$ . The wave number k is normalized to  $2\pi/\lambda_{L0}$  and the spectral intensity is normalized to the maximum intensity. The SRS signal is marked by the white dotted box.

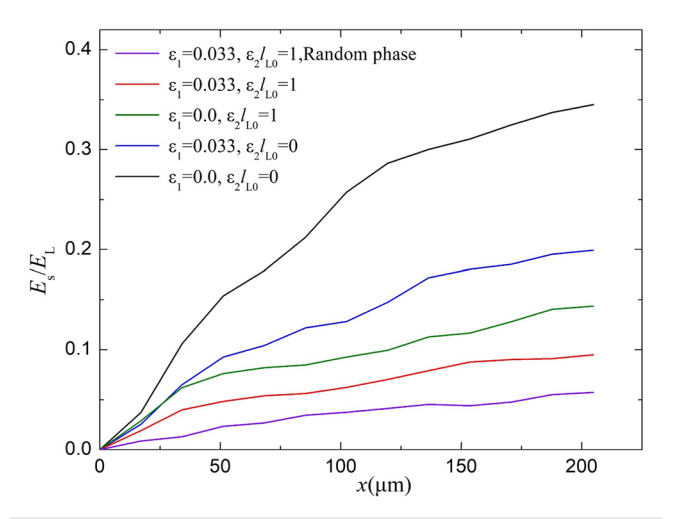


**FIG. 2.** Maximum field ratio  $\eta_S=E_s/E_L$  between SRS and driving pulses along the laser propagation direction for cases with different  $\Delta\omega$  and  $\Delta l$ : black line, LG case  $\varepsilon_1=0$ ,  $\varepsilon_2 l_{L0}=0$ ; blue line, LG case  $\varepsilon_1=0.033$ ,  $\varepsilon_2 l_{L0}=0$ ; green line, LS case  $\varepsilon_1=0$ ,  $\varepsilon_2 l_{L0}=1$ ; red line, LS case of  $\varepsilon_1=0.033$ ,  $\varepsilon_2 l_{L0}=1$ ; purple line, super LS case  $\varepsilon_1=0.033$ ,  $\varepsilon_2 l_{L0}=1$  together with random phases.

dominates the suppression of instabilities. We have also performed the simulations for a laser composed of Gaussian pulses at multiple frequencies, and the results are similar to those in the case of a broadband LG pulse and there is less of a suppressive effect than in the case of an LS pulse with  $\Delta l$  incoherence.

To clearly observe the growth process of SRS due to  $\Delta l$ , we plot in Fig. 2 the maximum field ratio between the SRS and the driving pulses along the laser propagation direction for different cases of  $\Delta \omega$  and  $\Delta l$ . The maximum field ratio is denoted by  $\eta_S = E_s/E_L$ , where  $E_s$  and  $E_L$  are the maximum fields of the SRS and driving pulses, respectively. From Fig. 2, we can observe the following. First,  $\eta_S$  is highest for  $\varepsilon_1 = 0$  and  $\varepsilon_2 l_{L0} = 0$ , indicating that this case has the most serious SRS for an LG pulse with a single frequency and a single topological charge. Second, at  $\varepsilon_2 l_{L0} = 0$ , i.e., with a single topological charge,  $\eta_S$  at 200  $\mu$ m decreases from 0.36 in the narrowband case ( $\varepsilon_1 = 0$ ) to 0.2 in the broadband case ( $\varepsilon_1 = 0.033$ ). This means that, as is well known, the use of a broadband pulse can help to suppress SRS. Third, keeping the same frequency band, we compare the LS

case ( $\varepsilon_2 l_{L0} = 1$ ) and the LG case ( $\varepsilon_2 l_{L0} = 0$ ). As can be seen, in the narrowband case ( $\varepsilon_1 = 0$ ),  $\eta_S$  at 200  $\mu$ m drops from 0.36 for the LG pulse to 0.15 for the LS pulse; and for the broadband case ( $\varepsilon_1 = 0.033$ ),  $\eta_S$  drops from 0.2 for the LG pulse to 0.05 for the LS pulse with random phase. These results indicate that the angular spread  $\Delta l$  can strongly suppress SRS growth.

It should be noted here that if a laser is composed of several beamlets with the same frequency but different topological charges, such as in the case of  $\varepsilon_1 = 0$  and  $\varepsilon_2 l_{L0} = 1$ , then the pitch of the LS pulse is infinite. This implies that the strong point with the highest intensity remains unchanged in the transverse direction. However, as shown in Fig. 2, SRS can still be suppressed to some degree, even though the peak intensity is much larger than that for an LG pulse. This strongly supports our idea that the spread of the angular momentum of the laser plays an important role in suppressing SRS. In addition, from Eq. (11), we can see that the suppressive effect is positively correlated with  $\Delta l$ . This implies that the suppressive effect is stronger for larger  $\Delta l$ . It should be noted that a large  $\Delta l$  means that the (average) topological charge of the LS beam should also be large, which means that the transverse spot of the driving beam must be sufficiently large. However, the focal spot of the driving beam in ICF is usually several hundred micrometers in size, which is large enough compared with the 10  $\mu$ m spot that we considered above. Therefore, taking account of the practical manipulations involved in ICF, the results in the present paper will be applicable at larger  $\Delta l$ .

One concern is that the superimposition of the LG beamlets produces a strong point in space and time, which may produce extra hot electrons and generate unacceptable shock preheating and entropy in the ICF fuel. Thus, it is necessary to investigate whether an LS pulse may produce more hot electrons and a higher electron temperature than an LG pulse. Figure 3 compares the electron distributions in the plasma driven by LG and LS pulses, respectively. Here, the plasma wave has still not completely decayed. It can clearly be seen that the LS pulse does not produce a high temperature or more hot electrons. Thus, the spread of the angular momentum of the LG pulse does not give rise to extra hot electrons. It should also be noted that SRS is a relatively long-term behavior in laser-plasma interaction. Here, we have considered relatively short pulses of 93.3 fs to save computational time. To avoid artificial results, we have carried out an additional PIC simulation for a longer duration of 186.6 fs, and this also shows a clear suppressive effect and a similar growth

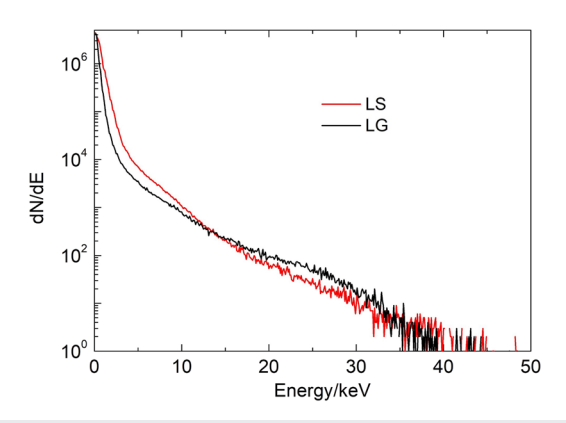


**FIG. 3.** Electron energy spectra when the driving laser pulse reaches x=240  $\mu m$  for an LG pulse with topological charge I=6 and  $\varepsilon_1=0.033$  (black line) and an LS pulse with topological charge varying from I=3 to I=9 and  $\varepsilon_1=0.033$  (red line).

In a laser facility, several laser beamlets are usually clustered into a laser bundle, which is used to drive a target. This makes it possible to change the beamlets from the usual Gaussian pulses to LG pulses with different topological charges and combine them into a super LS pulse with a spread topological charge. As shown in Fig. 4, an LS pulse can be produced by clustering obliquely incident LG beams of different frequencies  $\omega_L$  and topological charges  $l_L$  owing to the changing thickness of the phase plate azimuthally. The incident angles  $\theta$  of each incident LG beam relative to the x axis as shown in Fig. 4 differ slightly, owing to the small differences between the distances from the beamlets to the center of the source field plane. The pitch of the LS pulse is  $\Delta x = 2\pi c/(\omega_{L0}\varepsilon_1)$ , with  $\omega_{L0}\varepsilon_1 = \Delta\omega/\Delta l$ . For large laser facilities, it is at present still very difficult to control the relative phases of the beamlets. This implies that  $\phi_n$  is not the same for different LG pulses. Therefore, we usually obtain a super LS because of the random phase. Although this has several strong points

instead of a single perfect one, the spread of the angular momentum remains. The lowest growth rate is obtained in this case owing to the additional spatial incoherence, as shown in Fig. 2.

In a laser facility, we can create super LS bundles with incoherence in all dimensions of time, space, and angle by combining LG beamlets. By controlling the phases and frequencies of these beamlets before their combination, we can finally obtain the following three cases of the LS bundle, as shown in Fig. 4: (a) LS light with long pitch, which is narrowband, with one strong point of time-independent intensity; (b) LS light of short pitch, which is broadband, with one strong point of time-dependent intensity; (c) super LS light, with several strong points of time-dependent intensity owing to the random phase. Our results for these three cases confirm that angular incoherence clearly reduces the instability growth rate, with the suppressive effect of the super LS light being the most significant and even much stronger than that of temporal incoherence.

In summary, using both theoretical analysis and 3D PIC simulations, we have demonstrated the ability of an LS pulse with angular incoherence to suppress SRS in a plasma, which is of great significance for laser-driven ICF. According to our analytical study and simulations, angular incoherence has a much stronger suppressive effect on the instability growth rate than the temporal incoherence that is typically used. In particular, it is the angular momentum spread that plays an important role instead of the topological charge in suppressing instabilities. In other words, little suppression of SRS is achievable by only increasing the topological charge. In addition, it is interesting to note that the LS pulse does not generate additional hot electrons. It should be noted that in the simulations in this paper, we have considered the suppression of SRS as a specific example, but our conclusions can be applied to the suppression of SBS and other parametric instabilities. In a laser system, laser bundles of a super LS pulse can be generated by combining LG laser beamlets with different frequencies, different topological charges, and slightly different incidence angles, which can be produced from Gaussian beamlets using different phase plates. Our work has revealed a novel way to suppress LPI using light with angular incoherence, and it should

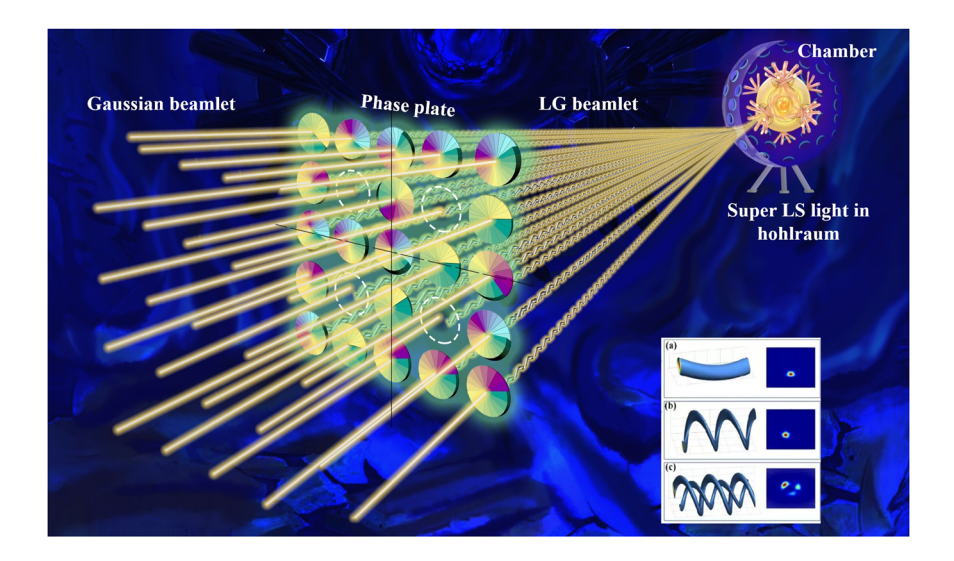


FIG. 4. Schematic of the generation of super LS light in a hohlraum at the center of a target chamber, by combining LG beamlets with different frequencies, different topological charges, and slightly different incidence angles, which are produced from Gaussian beamlets by using different phase plates. By controlling the phase and frequency of the LG beamlets via phase plates, we can obtain the following three cases at the observation plane: (a) LS of long pitch, (b) LS of short pitch, and (c) super LS.

be feasible to construct a low-LPI laser system by using super LS pulses with incoherence in all dimensions of time, space, and angle corresponding respectively to energy (frequency), momentum, and angular momentum. This may pave the way toward a low-LPI laser system for achieving predictable and reproducible fusion at high gain and may open the door to the use of longer-wavelength lasers for inertial fusion energy.

This work was supported by the National Key R&D Program of China (Grant No. 2018YFA0404803) and the National Natural Science Foundation of China (Grant Nos. 11922515, 11935008, 11335013, and 12035002).

#### **AUTHOR DECLARATIONS**

#### **Conflict of Interest**

The authors have no conflicts to disclose.

#### **Author Contributions**

Yi Guo: Data curation (equal); Methodology (equal); Writing – original draft (equal). Xiaomei Zhang: Resources (equal); Writing – original draft (equal); Writing – review & editing (equal). Dirui Xu: Data curation (equal); Formal analysis (equal). Xinju Guo: Methodology (equal); Software (equal). Baifei Shen: Conceptualization (equal); Supervision (equal); Writing – original draft (equal); Writing – review & editing (equal). Ke Lan: Conceptualization (equal); Writing – review & editing (equal).

#### **DATA AVAILABILITY**

The data that support the findings of this study are available from the corresponding authors upon reasonable request.

#### **REFERENCES**

- <sup>1</sup>J. Lindl, "Development of the indirect-drive approach to inertial confinement fusion and the target physics basis for ignition and gain," Phys. Plasmas 2, 3933–4024 (1995).
- <sup>2</sup>J. L. Kline, D. A. Callahan, S. H. Glenzer, N. B. Meezan, J. D. Moody, D. E. Hinkel, O. S. Jones, A. J. MacKinnon, R. Bennedetti, R. L. Berger *et al.*, "Hohlraum energetics scaling to 520 TW on the National Ignition Facility," Phys. Plasmas 20, 056314 (2013).
- N. T. Tikhonchuk, T. Gong, N. Jourdain, O. Renner, F. P. Condamine, K. Q. Pan, W. Nazarov, L. Hudec, J. Limpouch, R. Liska et al., "Studies of laser-plasma interaction physics with low-density targets for direct-drive inertial confinement fusion on the Shenguang III prototype," Matter Radiat. Extremes 6, 025902 (2021).
   S. Atzeni and J. Meyer-ter-Vehn, The Physics of Inertial Fusion (Oxford Science, Oxford, 2004).
- <sup>5</sup>R. Betti and O. A. Hurricane, "Inertial-confinement fusion with lasers," Nat. Phys. 12, 435–448 (2016).
- <sup>6</sup>K. Lan, "Dream fusion in octahedral spherical hohlraum," Matter Radiat. Extremes 7, 055701 (2022).
- <sup>7</sup>Y. Ping, V. A. Smalyuk, P. Amendt, R. Tommasini, J. E. Field, S. Khan, D. Bennett, E. Dewald, F. Graziani, S. Johnson *et al.*, "Enhanced energy coupling for indirectly driven inertial confinement fusion," Nat. Phys. 15, 138–141 (2019).
- <sup>8</sup>S. H. Glenzer, B. J. MacGowan, P. Michel, N. B. Meezan, L. J. Suter, S. N. Dixit, J. L. Kline, G. A. Kyrala, D. K. Bradley, D. A. Callahan *et al.*, "Symmetric inertial confinement fusion implosions at ultra-high laser energies," Science **327**, 1228–1231 (2010).

- <sup>9</sup>J. D. Lindl, P. Amendt, R. L. Berger, S. G. Glendinning, S. H. Glenzer, S. W. Haan, R. L. Kauffman, O. L. Landen, and L. J. Suter, "The physics basis for ignition using indirect-drive targets on the National Ignition Facility," Phys. Plasmas 11, 339–491 (2004).
- <sup>10</sup>J. D. Moody, P. Michel, L. Divol, R. L. Berger, E. Bond, D. K. Bradley, D. A. Callahan, E. L. Dewald, S. Dixit, M. J. Edwards *et al.*, "Multistep redirection by cross-beam power transfer of ultrahigh-power lasers in a plasma," Nat. Phys. 8, 344–349 (2012).
- <sup>11</sup> A. R. Christopherson, R. Betti, C. J. Forrest, J. Howard, W. Theobald, J. A. Delettrez, M. J. Rosenberg, A. A. Solodov, C. Stoeckl, D. Patel *et al.*, "Direct measurements of DT fuel preheat from hot electrons in direct-drive inertial confinement fusion," Phys. Rev. Lett. **127**, 055001 (2021).
- <sup>12</sup>J. Nilsen, A. L. Kritcher, M. E. Martin, R. E. Tipton, H. D. Whitley, D. C. Swift, T. Döppner, B. L. Bachmann, A. E. Lazicki, N. B. Kostinski *et al.*, "Understanding the effects of radiative preheat and self-emission from shock heating on equation of state measurement at 100s of Mbar using spherically converging shock waves in a NIF hohlraum," Matter Radiat. Extremes 5, 018401 (2020).
- <sup>13</sup>Y. Gao, Y. Cui, L. Ji, D. Rao, X. Zhao, F. Li, D. Liu, W. Feng, L. Xia, J. Liu *et al.*, "Development of low-coherence high-power laser drivers for inertial confinement fusion," Matter Radiat. Extremes 5, 065201 (2020).
- <sup>14</sup>B. J. Albright, L. Yin, and B. Afeyan, "Control of stimulated Raman scattering in the strongly nonlinear and kinetic regime using spike trains of uneven duration and delay," Phys. Rev. Lett. 113, 045002 (2014).
- <sup>15</sup>S. Skupsky, R. W. Short, T. Kessler, R. S. Craxton, S. Letzring, and J. M. Soures, "Improved laser-beam uniformity using the angular dispersion of frequency-modulated light," J. Appl. Phys. 66, 3456–3462 (1989).
- <sup>16</sup>E. Lefebvre, R. L. Berger, A. B. Langdon, B. J. MacGowan, J. E. Rothenberg, and E. A. Williams, "Reduction of laser self-focusing in plasma by polarization smoothing," Phys. Plasmas 5, 2701–2705 (1998).
- <sup>17</sup>J. D. Moody, B. J. MacGowan, J. E. Rothenberg, R. L. Berger, L. Divol, S. H. Glenzer, R. K. Kirkwood, E. A. Williams, and P. E. Young, "Backscatter reduction using combined spatial, temporal, and polarization beam smoothing in a long-scale-length laser plasma," Phys. Rev. Lett. 86, 2810–2813 (2001).
- <sup>18</sup>G. Cristoforetti, S. Hüller, P. Koester, L. Antonelli, S. Atzeni, F. Baffigi, D. Batani, C. Baird, N. Booth, M. Galimberti et al., "Observation and modelling of stimulated Raman scattering driven by an optically smoothed laser beam in experimental conditions relevant for shock ignition," High Power Laser Sci. Eng. 9, e60 (2021).
- <sup>19</sup>J. J. Thomson and J. I. Karush, "Effects of finite-bandwidth driver on the parametric instability," Phys. Fluids 17, 1608–1613 (1974).
- <sup>20</sup>S. P. Obenschain, N. C. Luhmann, and P. T. Greiling, "Effects of finite-bandwidth driver pumps on the parametric-decay instability," Phys. Rev. Lett. **36**, 1309–1312 (1976).
- <sup>21</sup>P. N. Guzdar, C. S. Liu, and R. H. Lehmberg, "The effect of bandwidth on the convective Raman instability in inhomogeneous plasmas," Phys. Fluids B 3, 2882–2888 (1991).
- <sup>22</sup>E. S. Dodd and D. Umstadter, "Coherent control of stimulated Raman scattering using chirped laser pulses," Phys. Plasmas 8, 3531–3534 (2001).
- <sup>23</sup> J. E. Santos, L. O. Silva, and R. Bingham, "White-light parametric instabilities in plasmas," Phys. Rev. Lett. 98, 235001 (2007).
- <sup>24</sup>Y. Zhao, L.-L. Yu, J. Zheng, S.-M. Weng, C. Ren, C.-S. Liu, and Z.-M. Sheng, "Effects of large laser bandwidth on stimulated Raman scattering instability in underdense plasma," Phys. Plasmas 22, 052119 (2015).
- <sup>25</sup>Y. Zhao, S. Weng, M. Chen, J. Zheng, H. Zhuo, C. Ren, Z. Sheng, and J. Zhang, "Effective suppression of parametric instabilities with decoupled broadband lasers in plasma," Phys. Plasmas 24, 112102 (2017).
- <sup>26</sup>Y. Zhao, S. Weng, Z. Sheng, and J. Zhu, "Suppression of parametric instabilities in inhomogeneous plasma with multi-frequency light," Plasma Phys. Controlled Fusion **61**, 115008 (2019).
- <sup>27</sup>H. H. Ma, X. F. Li, S. M. Weng, S. H. Yew, S. Kawata, P. Gibbon, Z. M. Sheng, and J. Zhang, "Mitigating parametric instabilities in plasmas by sunlight-like lasers," Matter Radiat. Extremes **6**, 055902 (2021).
- <sup>28</sup>Y. Zhao, Z. Sheng, Z. Cui, L. Ren, and J. Zhu, "Polychromatic drivers for inertial fusion energy," New J. Phys. **24**, 043025 (2022).

- <sup>29</sup> E. M. Campbell and W. J. Hogan, "The National Ignition Facility—Applications for inertial fusion energy and high-energy-density science," Plasma Phys. Controlled Fusion 41, B39–B56 (1999).
- <sup>30</sup>S. W. Haan, J. D. Lindl, D. A. Callahan, D. S. Clark, J. D. Salmonson, B. A. Hammel, L. J. Atherton, R. C. Cook, M. J. Edwards, S. Glenzer *et al.*, "Point design targets, specifications, and requirements for the 2010 ignition campaign on the National Ignition Facility," Phys. Plasmas 18, 051001 (2011).
- <sup>31</sup> A. B. Zylstra, A. L. Kritcher, O. A. Hurricane, D. A. Callahan, J. E. Ralph, D. T. Casey, A. Pak, O. L. Landen, B. Bachmann, K. L. Baker *et al.*, "Experimental achievement and signatures of ignition at the National Ignition Facility," Phys. Rev. E **106**, 025202 (2022).
- J. Lindl, O. Landen, J. Edwards, E. Moses, and N. Team, "Review of the National Ignition Campaign 2009-2012," Phys. Plasmas 21, 020501 (2014).
   National Nuclear Security Administration, "2015 review of the inertial confine-
- <sup>33</sup>National Nuclear Security Administration, "2015 review of the inertial confinement fusion and high energy density science portfolio: Volume I," Report No. DOE/NA-0040, May 2016.
- <sup>34</sup>Lawrence Livermore National Laboratory, "Lasers indirect drive input to NNSA 2020 report," Report No. LLNL-TR-810573, May 2020.
- 35 J. Tollefson and E. Gibney, "Nuclear-fusion lab achieves 'ignition': What does it mean?," Nature 612, 597–598 (2022).
- <sup>36</sup>J. T. Mendonça, B. Thidé, and H. Then, "Stimulated Raman and Brillouin backscattering of collimated beams carrying orbital angular momentum," Phys. Rev. Lett. 102, 185005 (2009).

- <sup>37</sup>R. Nuter, P. Korneev, and V. T. Tikhonchuk, "Raman scattering of a laser beam carrying an orbital angular momentum," Phys. Plasmas **29**, 062101 (2022).
- <sup>38</sup> J. Vieira, R. M. G. M. Trines, E. P. Alves, R. A. Fonseca, J. T. Mendonça, R. Bingham, P. Norreys, and L. O. Silva, "Amplification and generation of ultra-intense twisted laser pulses via stimulated Raman scattering," Nat. Commun. 7, 10371 (2016).
- <sup>39</sup>J. A. Arteaga, A. Serbeto, K. H. Tsui, and J. T. Mendonça, "Light spring amplification in a multi-frequency Raman amplifier," Phys. Plasmas 25, 123111 (2018).
- <sup>40</sup>G. Pariente and F. Quéré, "Spatio-temporal light springs: Extended encoding of orbital angular momentum in ultrashort pulses," Opt. Lett. **40**, 2037–2040 (2015).
- <sup>41</sup> J. Vieira, J. T. Mendonça, and F. Quéré, "Optical control of the topology of laser-plasma accelerators," Phys. Rev. Lett. **121**, 054801 (2018).
- <sup>42</sup>J. F. Drake, P. K. Kaw, Y. C. Lee, G. Schmid, C. S. Liu, and M. N. Rosenbluth, "Parametric instabilities of electromagnetic waves in plasmas," Phys. Fluids 17, 778–785 (1974).
- <sup>43</sup>D. W. Forslund, J. M. Kindel, and E. L. Lindman, "Theory of stimulated scattering processes in laser-irradiated plasmas," Phys. Fluids **18**, 1002–1016 (1975).
- <sup>44</sup>T. D. Arber, K. Bennett, C. S. Brady, A. Lawrence-Douglas, M. G. Ramsay, N. J. Sircombe, P. Gillies, R. G. Evans, H. Schmitz, A. R. Bell, and C. P. Ridgers, "Contemporary particle-in-cell approach to laser-plasma modelling," Plasma Phys. Controlled Fusion 57, 113001 (2015).